

ARTICLE

Supported Ionic Liquid-Like Phases as efficient solid ionic solvent for the immobilisation of alcohol dehydrogenases towards the development of stereoselective bioreductions

Received 00th January 20xx,
Accepted 00th January 20xx

DOI: 10.1039/x0xx00000x

Raul Porcar,^{a,d} Iván Lavandera,^b Pedro Lozano,^c Belen Altava,^a Santiago V. Luis,^a Vicente Gotor-Fernández,^{*b} and Eduardo García-Verdugo^{*a}

Polymeric material containing ionic liquid fragments, like those found in bulk ILs, are excellent solid media for the immobilisation of biocatalysts. Herein, the entrapment of the enzymatic system formed by alcohol dehydrogenase from *Rhodococcus ruber* (ADH-A) overexpressed in *E. coli* and its coenzyme has been studied. The activity, stability and reusability of these preparations have been investigated in the bioreduction of prochiral ketones finding excellent levels of conversion and selectivity. Interestingly, the immobilised enzyme remained active and exhibited excellent stability in aqueous solutions after several recycling uses. More importantly, these biopolymer materials retained most of their activity after consecutive reaction cycles, prolonged storage and under flow conditions.

Introduction

Solvent choice is a key parameter in organic chemistry reactions since it can directly interact with catalysts, substrates and products, all these interactions displaying a remarkable influence in the reaction rate and/or the selectivity, but also facilitating or hampering product isolation.¹ In the case of biotransformations, the proper selection of the solvent is essential in terms of enzyme activity leading in some cases to a partial or total deactivation when the wrong combination is selected. These effects are maximised when Ionic Liquids (ILs) are used as reaction media for enzyme-catalysed transformations.²

ILs exhibit physicochemical properties, which can be modulated considering a myriad of structural modifications at the cation or anion properties.³ Thus, ILs can be considered as “*design media*” whose physical and chemical properties can be adjusted at the molecular level to enhance the (bio)catalytic properties.^{4,5} For instance, the over-stabilisation effect of ILs on enzymes,⁶ and their successful combination for synthetic purposes has been elegantly reviewed in recent years.⁷

The physical adsorption of ILs onto solid supports (Supported Ionic Liquid Phases: SILPs) has been envisioned to mitigate

some of the drawbacks associated to the application of ILs in (bio)catalytic processes (i.e. high cost, complex separations or some (eco)toxicological concerns).^{8,9} Thus, SILPs/scCO₂ biphasic systems have been extensively used for developing biotransformations under continuous flow conditions.¹⁰ SILPs, however, have the limitation, especially for continuous processes, of the potential lixiviation of the IL or the catalyst by abrasion and dissolution. As suitable alternative, the covalent functionalisation of solid polymeric surfaces with IL-like moieties (Supported Ionic Liquid-Like Phases: SILLPs) has been developed.¹¹ The IL-like units provide to these advanced materials with the main features of molecular ILs (stability, tuneable polarity, nanostructure, etc.),^{12,13} while the cross-linked backbones offer an additional design vector to optimize their macroscopic and process properties.

These SILLPs present some advantages themselves when applied as “*self-organised solid ionic solvents*” for catalytic processes, providing similar features than bulk ILs but simplifying product isolation and recycling of the catalyst-IL-phase as well as alleviating (eco)toxicological concerns.¹⁴ In a similar way to liquid IL-phases, SILLPs can also be used to fine-tune the catalyst performance assisting the activation of the catalyst, generating novel catalytic species, improving its stability and influencing the (stereo)selectivity. SILLPs have been applied to a wide range of catalysts including metal nanoparticles,¹⁵ photocatalysts,¹⁶ organometallic catalysts,¹⁷ enzymes,¹⁸ and organocatalysts.¹⁹ Furthermore, the efficiency of these systems can be further improved by the development of continuous flow processes as an additional enabling technology, which reduces product inhibition issues, facilitating the downstream process (i.e. by using supported enzymes) and improving the total process productivity (Total turnover numbers, TNNs) as well as allowing the combination

^aDpt. of Inorganic and Organic Chemistry, Supramolecular and Sustainable Chemistry Group, University Jaume I, Avda Sos Baynat s/n, E-12071. Castellon, Spain.

^bOrganic Chemistry Department. University of Oviedo. Avenida Julián Clavería, E-33006. Oviedo, Spain.

^cFacultad de Química, Universidad de Murcia, Dep. Bioquímica y Biología Molecular “B” e Inmunología, Campus de Espinardo, E-30100. Murcia, Spain.

^dDepartamento de Química Orgánica y Bio-Orgánica, Facultad de Ciencias, UNED, Avenida de Esparta s/n, 28232. Las Rozas-Madrid, Spain.

See DOI: 10.1039/x0xx00000x

in one reactor with organometallic, photocatalyst or organocatalytic systems in cascade systems.¹⁰

ADHs have attracted great attention because of their ability to catalyse highly selective reductions of carbonyl groups in, e.g., aldehydes, ketones, or keto esters.²⁰ ADHs have been also used in ILs,⁶ however, their activity in water-immiscible ILs systems (e.g. [Bmim][NTf₂], [Bmim][PF₆]) was lower than that in aqueous media.²¹ Thus, aqueous buffer/IL biphasic systems have been applied to carry out the enantioselective reduction of ketones (e.g. 2-octanone) in the aqueous phase, coupled with the extraction of the *sec*-alcohol product (e.g. 2-octanol) in the IL phase, due to favourable partition coefficients.²²

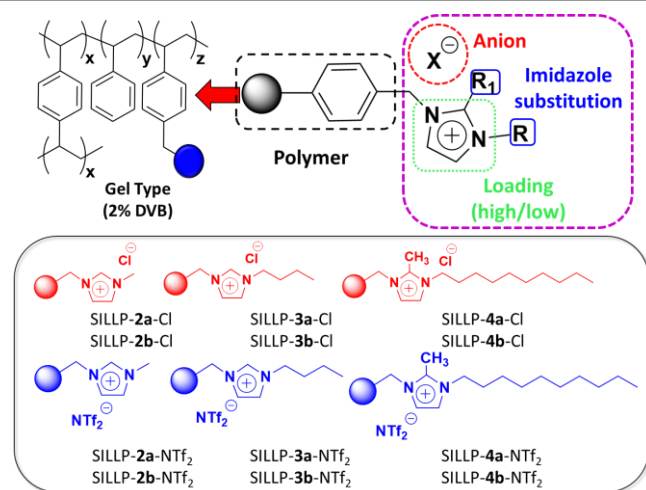


Figure 1. Supported ionic liquid tested for the immobilisation SILLPs 1-4a-b.

Alternatively, water-miscible ILs based in hydroxy-functionalised ‘Tris-like’-cation (e.g. ammoeng™ 100, TEGO™ IL K5, etc) were successfully employed in monophasic systems for the ADH/NADH redox couple-catalysed enantioselective reduction of aliphatic ketones,²¹ even integrated in membrane reactor for product separation with excellent operational stability (i.e. up to 99.9 enantioselectivity for 1000 h operation).²³ In this context, studies dealing with their immobilisation of advanced materials based on ILs are scarcely reported being mainly focused in the development of supported bioelectrode for analytic applications.²⁴

This work reports the application of supported ionic liquid phases as suitable non-conventional solid ionic solvents for immobilisation of redox biocatalytic systems. The redox couple consisting in an alcohol dehydrogenase enzyme (ADHs, also called ketoreductases or carbonyl reductases) and nicotinamide adenine dinucleotide (NAD) coenzyme has been used as representative example, resulting in an enhancement in activity under continuous operation. Particularly, the NAD-dependent ADH-A from *Rhodococcus ruber* DSM 44541²⁵ was selected for this investigation, since its overexpression on *E. coli* cells provides multiple advantages in terms of (organic) solvents tolerance,²⁶ and simple use for synthetic stereoselective purposes.²⁷

Results and Discussion

Immobilisation of ADH-A/NADH redox system onto SILLPs. A series of twelve different SILLPs (Fig. 1) were selected to evaluate the immobilisation of lyophilised *E. coli* cells overexpressing ADH-A, which displays Prelog selectivity (Fig. 1). Up to now, there is just one contribution from Kroutil and Liese related to the immobilisation of this biocatalyst following a covalent strategy on porous glass beads.²⁸ This allows us evaluating simultaneously three different SILLPs design vectors. In the first place, the loading of SILLPs was considered. Thus, Merrifield-type polymer (gel-type polystyrene-divinylbenzene, PS-DVB, with 2% crosslinking) with different loadings were used for the SILLPs preparation, where **a** state for high loading (ca. 4.3 meq Cl/g), and **b** for low loading (ca. 1.1 meq Cl/g). A second design vector was the substitution pattern of the imidazolium cation. SILLPs based on methyl (**2a,b**), butyl (**3a,b**) and 1-decyl-2-methyl imidazolium (**4a,b**) were synthesised by grafting of the corresponding alkyl-imidazole onto the commercial Merrifield gel type resins with high and low loading.²⁹ Finally, both hydrophilic (Cl⁻) and hydrophobic (NTf₂⁻) anions were alternatively used. The immobilisation of the biocatalyst was carried out by simple adsorption of the ADH/NAD redox system onto the SILLPs by incubating the corresponding support (1 g) with 25 mL of an aqueous suspension of lyophilised cells of *E. coli*-ADH-A (4 mg/mL, Fig. 2a).³⁰ Then, the SILLPs were filtered and lyophilised leading to the corresponding immobilised ADH-SILLPs catalytic systems.

Evaluation of the ADH-SILLP system. The ability of these systems to catalyse the reduction of acetophenone (**5a**) to the corresponding (*S*)-1-phenylethanol (**6a**) was firstly assayed as benchmark reaction (Fig. 2). In all the cases, the reaction was carried out at 40 mM substrate concentration using a 50 mM Tris-HCl buffer pH 7.6 and the same weight of polymer independently of the protein loading. To drive the equilibrium towards the alcohol product formation and with nicotinamide cofactor recycling purposes, a ‘coupled-substrate’ approach using inexpensive propan-2-ol (isopropanol, IPA) as hydrogen donor (co-substrate). Gratifyingly, all the assayed supported enzymes were able to catalyse the selective formation of (*S*)-1-phenylethanol with complete selectivity (>99% *ee*).

Interestingly, the conversion values varied depending on the nature of the SILLPs used for the immobilisation (Fig. 2b). In general, the supports bearing a high loading of IL-like units were more active than those with a lower loading. The nature of the counterion also played a key role. Thus, the presence of a hydrophobic anion (NTf₂⁻) led to a lower catalytic efficiency (less of 25% conversion) in comparison with the chloride ones (up to 80%). Only in the case of ADH-SILLP-**3a**-NTf₂ (high loading IL-like units and methyl imidazolium), which is the most hydrophilic among the hydrophobic SILLPs, a slightly better conversion was observed (23% conversion). Higher conversions were obtained for the more hydrophilic resins, especially for those SILLPs with high loading of IL-like units, which reached ca. of 80% of conversion into (*S*)-**6a**.³¹ These initial results demonstrated the excellent suitability of SILLPs

to be used to produce active supported oxidoreductases, because they maintain the excellences of the bare ILs on the enzyme microenvironment, as previously demonstrated by

homogenous ILs.⁶ Our initial results, also suggest that the hydrophilic/hydrophobic balance of the support is essential to achieve an efficient immobilised biocatalyst.

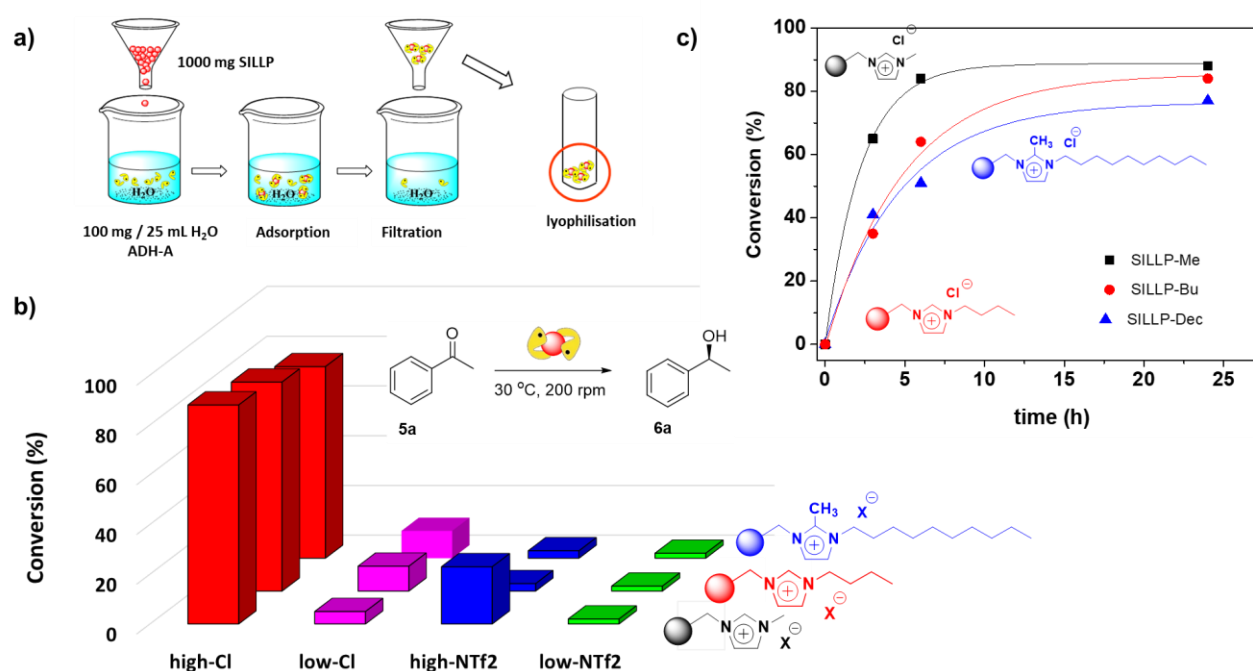


Figure 2. a) Schematic immobilisation of ADH-A into different SILLPs. b) Screening of ADH-SILLPs composites (50 mg) in the bioreduction of acetophenone (**5a**, 40 mM) using IPA (0.68 M) in a 50 mM Tris-HCl buffer pH 7.6 at 200 rpm and 30 °C. c) Conversion vs time profiles obtained in the bioreduction of acetophenone (40 mM) catalysed by ADH-SILLPs composites (50 mg) using IPA (0.68 M) in 50 mM Tris-HCl buffer pH 7.6 at 30 °C and 200 rpm. ADH-SILLP-**2a**-Cl (square), ADH-SILLP-**3a**-Cl (dot) and ADH-SILLP-**4a**-Cl (triangle).

In a more detailed study, the bioreduction of acetophenone was further investigated using the more active ADH-SILLPs systems (ADH-SILLP-**2-4a**-Cl, Fig. 2c), which were monitored with time. After 24 h, the three biocatalysts led to similar conversions (70-80%), obtaining in all cases (*S*)-**6a** in enantiopure form. The catalytic efficiency of these systems was clearly influenced by the substitution pattern of the imidazolium cation. This difference on activity can be related with the enzymatic loading. Thus, to calculate it, these three active ADH-SILLPs systems were suspended in an aqueous NaCl 0.2 M solution to desorb the immobilised protein. The Bradford assay of the supernatant allowed us to calculate the protein loading. Noteworthy, the amount of protein immobilised was significantly low, in the range of 32-42 $\mu\text{g/g}$ of SILLPs (Table 1). At the view of these results, the differences on activity observed cannot be attributed at different protein loading. Indeed, the supported biocatalytic system ADH-SILLP-**3a**-Cl with slightly higher protein loading (42.3 $\mu\text{g/g}$ of SILLP) was the less active. The ADH-SILLP-**2a**-Cl bearing methyl imidazolium IL-like units showed higher activity than the other two systems with a specific activity of $2.04 \times 10^5 \mu\text{mol alcohol} \times \text{h}^{-1} \times \text{mg Enz}^{-1}$ (Table 1).

Table 1. Enzymatic loading and specific activity.^[a]

Entry	SILLPs	Protein Loading ^[b]	Swelling ^[c]	Specific Activity ^[d]
1	ADH-SILLP- 2a -Cl	32.4	47	$2.04\text{E}+05$
2	ADH-SILLP- 3a -Cl	38.9	40	$8.58\text{E}+04$
3	ADH-SILLP- 4a -Cl	42.3	14	$8.58\text{E}+04$

[a] 100 mg of *E. coli*/ADH-A lyophilised cells were added to a suspension of 1000 mg of the support in 25 mL Milli-Q H₂O. [b] immobilised protein per g support, calculated by Bradford assay as $\mu\text{g protein/g SILLP}$. [c] Diameter increase (%) upon swelling in water. [d] $\mu\text{mol alcohol} \times \text{h}^{-1} \times \text{mg protein}^{-1}$.

The activity differences may be associated with the hydrophilic/hydrophobic balance provided by the presence and nature of the IL-like moieties. It should be considering that the starting Merrifield resins are highly hydrophobic as corresponds to the presence of the PS-DVB polymeric backbone.^{12,29} In fact, the unmodified Merrifield resin shrank when suspended in water (-5% diameter change). However, upon the modification with the IL-like moieties the resins become hydrophilic.^{12,29} Those SILLPs are now compatible with water and the corresponding gel-type polymers swell at an appreciable extent in aqueous medium. Swelling is an

important property to allow the access of the reactants to the enzyme active site, so keeping the biocatalyst in an aqueous environment is ideal to preserve its activity along the time. Remarkably, the swelling degree of the SILLPs highly depends on the imidazolium substitution pattern, Table 1 displaying the values achieved for the studied systems. For instance, swelling in water for ADH-SILLP-**2a**-Cl, as measured by the increase in diameter, is almost 50% (Entry 1, Table 1). The increased of the hydrophobic character (decyl > butyl > methyl) of the IL-like moieties led to a reduction of the swelling in the order (ADH-SILLP-**2a**-Cl > ADH-SILLP-**3a**-Cl > ADH-SILLP-**4a**-Cl). This swelling trend matches with the drop of biocatalytic activity. This effect is even more important in the case of ADH-SILLPs systems where NTf₂ is used as counterion since this anion significantly reduces the hydrophilic character of the supports and their swelling, obviously leading to a significant decrease of the catalytic activity.

Table 2. Recover activity vs amount of DMSO used as co-solvent, including also enzyme recycling studies.^[a]

Entry	DMSO (%) ^[b]	Recover Activity (%) ^[c]
1	0	100
2 ^[d]	0	60
3 ^[e]	0	95
4	10	99
5	20	99
6	30	78
7	100	5

[a] ADH-SILLP-**2a**-Cl (50 mg), acetophenone (**5a**, 38 mM) solution in a 50 mM Tris-HCl buffer pH 7.6 (636 μ L), IPA (0.68 M) and DMSO (0-100% v/v). [b] Percentage of v/v DMSO in the buffer:DMSO mixture. [c] Recover activity = conversion / conversion under standard conditions: entry 1 (89% conversion into (*S*)-**6a** with >99% ee). [d] 2nd use under the same experimental conditions. [e] 3rd use under standard conditions with addition of NADH (0.73 mM).

Stability study and co-solvent tolerance. The stability of the supported biocatalyst upon consecutive uses is a key factor for the practical application of these systems. Thus, to test the stability of the immobilised enzyme, the most active ADH-A preparation (ADH-SILLP-**2a**-Cl) was recovered after its use under standard conditions and assayed in a second cycle, displaying only a 60% of recovery of the initial activity (Entry 2, Table 2). This decrease on the activity is likely due to partial leaching of the NADH cofactor immobilised onto the SILLPs. The reason behind such leaching can be attributed to the reversible ionic interactions between the negatively charged phosphorylated cofactors and the positive charges of the solid material, establishing an association/dissociation equilibrium which permits the release of NADH cofactor molecules from the solid surface to the aqueous solution, especially when buffer systems are used.³² However, when the supported biocatalyst was tested in a third use, but with external addition of a fresh NADH (0.73 mM) solution, the system attained a similar recovered activity in comparison with the initial conditions (95%, Entry 3, Table 2). This experiment, demonstrates that the immobilised enzyme onto the SILLPs displayed a remarkable stability regardless cofactor leaching, allowing the reuse of the catalyst for practical applications.

Taking advantage of the high stability shown by this enzyme in the presence of high concentrations of organic solvents, we further evaluated the stability of the immobilised preparations and their compatibility with organic solvents,^{26,33} a series of experiments were performed testing increasing amounts of DMSO as co-solvent (Table 2, Entries 4-7). DMSO is not considered as an appropriate co-solvent for alcohol dehydrogenases,^{34,35} however, it can provide the advantage of solubilizing a wide variety of organic substrates, as most of them are highly hydrophobic displaying low solubility in aqueous media. To study the possible stabilisation effect of the SILLPs against DMSO, the recovery activity for the model reaction catalysed by ADH-SILLP-**2a**-Cl was measured at different DMSO/H₂O ratios (10-100% v/v). The biocatalyst showed a complete deactivation when the reaction was performed in pure DMSO (Entry 7, Table 2). However, total recovery activities (>99%) were achieved when 10% and 20% of DMSO were employed (Entries 4 and 5, Table 2), and even when the DMSO concentration was brought to 30%, a significant 78% value was achieved (Entry 6, Table 2).

Table 3. Enzymatic activity vs substrate **5a** concentration.^[a]

Entry	[5a] (mM)	DMSO (%) ^[b]	(%) ^[c]	Specific Activity ^[d]
1	40	0	86	102.8
2	51	9.1	85	129.6
3	71	16.7	76	161.3
4	99	23	71	210.2
5	233	43	10	69.7

[a] ADH-SILLP-**2a**-Cl, **5a** (40-233 mM) in a 50 mM Tris-HCl buffer pH 7.6 (636 μ L) with IPA (0.68 mM) and DMSO. [b] Percentage of DMSO in the mixture aqueous buffer:DMSO. [c] Conversion into (*S*)-1-phenylethanol calculated by GC. [d] Specific activity is defined as mg alcohol x mg protein⁻¹ x h⁻¹.

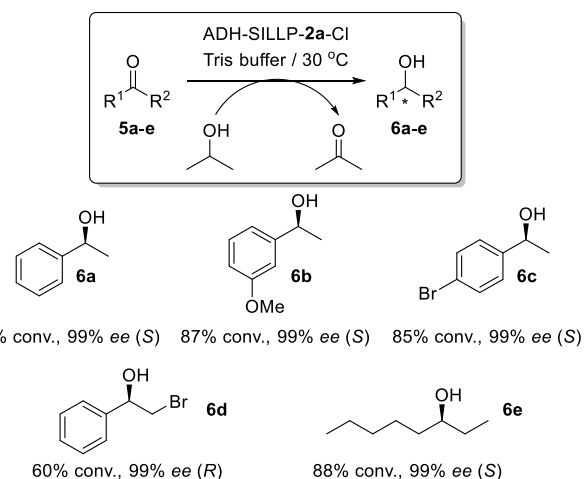


Figure 3. Stereoselective bioreductions of other ketone substrates using ADH-SILLP-**2a**-Cl. Conditions: 40 mM ketone and 0.68 M of IPA in Tris-HCl buffer pH 7.6, 200 rpm, 30 °C catalysed by 50 mg of ADH-SILLP-**2a**-Cl. Conversion and ee values calculated by GC.

In additional experiments, the use of higher acetophenone (**5a**) concentrations was investigated to improve the catalytic systems productivity (Table 3). To work at higher concentrations of **5a** ranging from a total 40 mM to 233 mM of

ketone, the amount of DMSO was successively increased (Table 3), interestingly finding a gradual but not dramatic loss of the enzymatic activity until 99 mM (71-86% conversion Entries 1-4, Table 3), while the activity dropped until 10% conversion when considering a 233 mM concentration (Entry 5, Table 3). The immobilised enzyme was highly tolerant to the organic solvent since when a 23% of DMSO was used for a 99 mM of **5a**, the conversion reached a 70% depicting the higher productivity ($161.3 \text{ mg alcohol} \times \text{mg Enz}^{-1} \times \text{h}^{-1}$).

Substrate scope. At this point and searching to expand the synthetic potential of the immobilised ADH-A preparation, the

activity and selectivity of the ADH-SILLP-**2a**-Cl were also evaluated for the bioreduction of different substrates, such as ketones **5b-e** (Fig. 3). The different assayed aromatic and aliphatic ketones showed reasonable activities (60-88% conversion) and excellent stereoselectivities (99% *ee*). In general, the reduction yielded the corresponding (*S*)-alcohols **6b,c,e**. In the case of the ketone **5d** the alcohol (*R*)-**6d** (due to a change in the CIP priorities), which is a key intermediate in the synthesis of pharmaceuticals for the treatment of obesity and depression, was obtained in enantiopure form and 60% conversion.³⁶

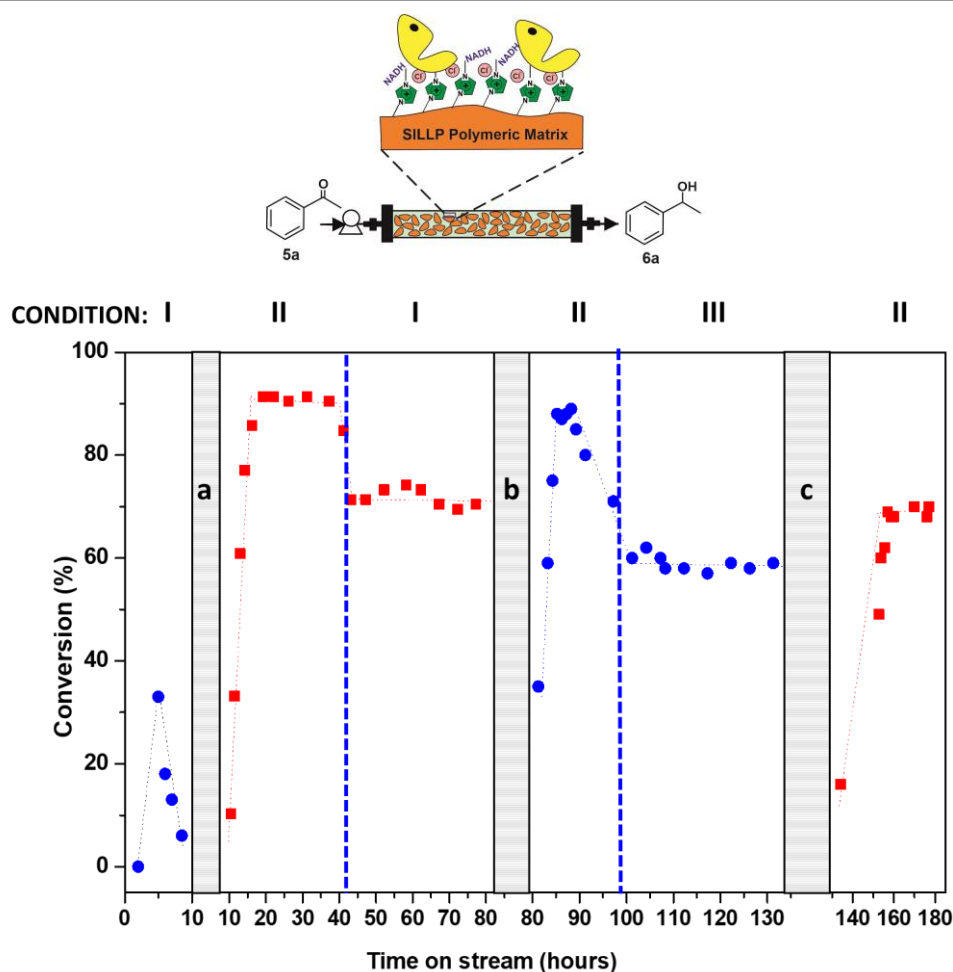


Figure 4. Schematic representation of the flow-through system. Conversion vs time on stream. They grey bars represent reaction breaks. During these breaks the reactor was washed with deionised water and stored at room temperature. Break a: overnight, Break b: 12 days of storage and Break c: 9 days. The bioreactor was operated at $50 \mu\text{L min}^{-1}$, pH 7.6 and at 30°C with the following conditions: I) **5a** (40 mM) in 50 mM Tris-HCl buffer pH 7.6 with a 12:1 v/v ratio IPA:**5a** without NADH; II) **5a** (40 mM) in 50 mM Tris-HCl buffer pH 7.6 with a 12:1 v/v ratio IPA:**5a** with NADH (0.73 mM); III) **5a** (40 mM) in 50 mM Tris-HCl 12:1 v/v IPA:**5a**, with 0.073 mM NADH.

Table 4. Reduction of **5a** under continuous flow conditions catalysed by immobilised ADH systems.^[a]

Entry	Biocatalysts/support	STY ($\text{g} \times \text{L}^{-1} \times \text{h}^{-1}$)	Stability	Reference
1	Lb-ADH onto cross-linked polyacrylic acid	7.5	Decay after 7 h of continuous use	37
2	Lb-ADH onto HaloTag-Sepharose® beads	43.1	32h without loss in performance	41
3	Lb-ADH onto HaloTag-Sepharose® beads	28.2	138 h without loss in performance	38
4	Lb-ADH onto aminoepoxy-Sepabead®	1.25	78 days without loss in performance	39
5	ADH-A onto PS-DVB-SILLPs	11.85	80h without loss in performance	This work

Evolution under continuous flow conditions. Continuous flow reactors represent optimal systems to evaluate the long-term stability of a given (bio)catalyst.⁴⁰ Therefore, to evaluate the stability of the immobilised ADH-A onto SILLPs, a fixed bed reactor was set-up. Fig. 4 depicts the results obtained to evaluate the performance of the biocatalyst ADH-SILLP-2a-Cl. Initially, a 40 mM solution of **5a** in 50 mM Tris-HCl buffer at pH 7.6 with IPA (0.74 M) was used without the addition of the nicotinamide cofactor NADH (Condition I, Fig. 4). The presence of a residual cofactor content in the raw enzyme source used for immobilization rendered modest level of activity reaching the conversion a value of *ca.* 37% at a flow of 50 $\mu\text{L min}^{-1}$. However, a strong activity decay was immediately observed, being as it is likely that the cofactor, co-immobilised during the preparation of the supported biocatalyst, was washed out by anion exchange with buffer continuously pumped through the reactor. After this first test, the reactor was washed and stored in buffer overnight at room temperature (a, Fig. 4). In the following experiment, a 40 mM solution of **5a** and 0.74 M of IPA in 50 mM Tris-HCl buffer pH 7.6 with NADH (0.73 mM) was pumped through the reactor (Condition II, Fig. 4). Under these conditions and after reaching the steady state, a conversion of *ca.* 90% was obtained, attaining similar conversion levels than the found under batch conditions. However, the Space Time Yield (STY) achieved for the flow system 22.6 $\text{g} \times \text{L}^{-1} \times \text{h}^{-1}$ was much higher than the achieved under batch conditions (1.976 $\text{g} \times \text{L}^{-1} \times \text{h}^{-1}$) proving that the continuous flow system help to enhance the efficiency of the process. The bioreactor showed a good stability with a steady productivity of 26.35 $\text{mg}_{(\text{Product})} \times \text{g}_{(\text{catalyst})}^{-1} \times \text{h}^{-1}$ for at least 24 h. After that period, NADH was removed from the feed solution, coming back to the condition I used in first experiment. Under these conditions, the conversion decreased taking a value around *ca.* 70%, which was significantly higher than the found under Condition I during the first experiment (only *ca.* 37%). Furthermore, this conversion was maintained for around 30 h suggesting that during the reaction in the presence of NADH (condition II), certain amount of the negatively charged phosphorylated cofactor may be attached onto the SILLP by ionic exchange with the positive charges of the solid material. Thus, the support is likely to act as cofactor reservoir establishing an association/dissociation equilibrium, which maintain certain level of cofactor molecules on the solid surface leading to a more active catalytic system.

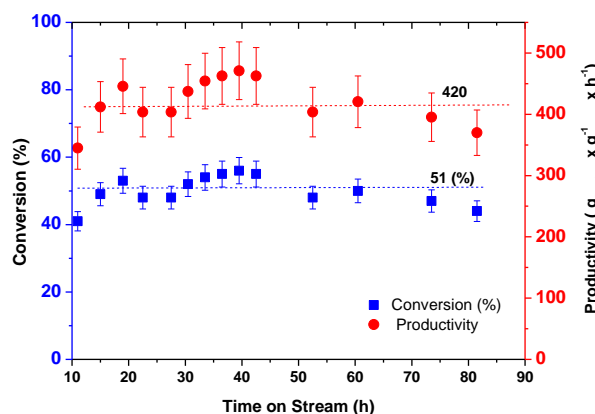


Figure 5. Conversion and productivity vs time on stream. The bioreactor was operated at 50 $\mu\text{L min}^{-1}$ flow at 30 $^{\circ}\text{C}$ with the following conditions: **5a** (71 mM) in 77.7:15.5:6.8 v/v 50 mM Tris-HCl buffer pH 7.6, DMSO:IPA, 12:1 v/v IPA:**5a** and NADH (1.3 mM).

After, this experiment the reactor was washed and stored at room temperature for 12 days (b, Fig. 4). In order, to evaluate if the system was still active after this period, the reaction was performed using the same conditions above reported (Condition II, Fig. 5). A conversion of *ca.* 87% was achieved after reaching the steady state. Thus, it has been demonstrated that the system remains still active after a long period of storage. Finally, an additional experiment was performed, adding ten-times less of NADH (0.073 mM). Under this condition III, the system was active and stable but only *ca.* 58% conversion was reached. Once again, after this experiment the reactor was washed and stored for 9 days (c, Fig. 4). However, after this period and using the conditions providing highest conversions (Condition II, Fig. 4) the system was not able to recover the full activity, reaching only *ca.* 68% of conversion. After all these experiments, we can conclude that ADH-SILLP-2a-Cl provides an active (90% conversion and 22.6 $\text{g} \times \text{L}^{-1} \times \text{h}^{-1}$) and stable system for asymmetric ketone bioreductions. Furthermore, the system shows a good stability keeping active during at least 5 days of continuous use and more than 25 days of use and storage. Overall, the SILLP-ADH preparations seem to be efficient immobilised systems, the addition of external NADH being required to maintain the high level of activity. As demonstrated by Pietruszka et al. under continuous flow conditions a closed-loop setup can be implemented for the recovery and re-use of the cofactor reducing the cost associated with it.⁴¹

To know the redox biocatalytic performance of this NAD-ADH-SILLP system, a more concentrate substrate solution (71 mM of **5a**), containing DMSO as cosolvent for full ketone solubilisation, was studied (Fig. 5). The system showed good stability for at least 3 days of continuous use. The mean space-time yield for this experiment was 11.85 $\text{g} \times \text{L}^{-1} \times \text{h}^{-1}$ corresponding with a mean conversion of 51% and a productivity of 420 $\text{g}_{\text{alcohol}} \times \text{g}_{\text{enzyme}}^{-1} \times \text{h}^{-1}$ and excellent

enantioselectivities (>99%). Thus, the TNN for hour of the system was $2.8 \times 10^5 \text{ mol}_{\text{alcohol}} \times \text{mol}_{\text{enzyme}}^{-1} \times \text{h}^{-1}$ corresponding with a TON for catalytic bed of $1.19 \times 10^5 \text{ mol}_{\text{alcohol}} \times \text{mol}_{\text{enzyme}}^{-1}$. Thus according with these parameters the ADH-SILLPs systems here developed can be classified attending to the recent publication by López-Gallego as low activity high stability ($\ln(\text{STY}) 2.47 \text{ g} \times \text{L}^{-1} \times \text{h}^{-1}$ and $\ln(\text{TON}) 11.7 \text{ mol}_{\text{alcohol}} \times \text{mol}_{\text{enzyme}}^{-1}$).⁴² The high stability displayed by the system can be attributed to the IL-like units as it is well-known that the IL can increase the stability of different enzyme classes.⁶ The low activity can be related with the low loading achieved (32.4 μg immobilised protein per g support) by adsorption. We are currently evaluating other types of immobilisation (i.e. entrapment) in order to improve the loading and therefore the catalytic activity and STY of these preparations.

The systems here reported are as far as we aware the first example of of *E. coli*/ADH-A immobilised into supported ionic liquid phases for the continuous flow asymmetric bioreduction of ketones. The efficiency of the resulting packing bed reactors showed a similar performance in terms of the productivity than other ADH immobilised onto conventional supports (Table 4). However, here the immobilisation was performed by simple adsorption onto the SILLPs and the presence of the IL-moieties allow to fine tune the activity of the resulting systems not achievable with conventional supports.

Conclusions

A simple immobilisation, without any further purification, of lyophilised *E. coli* cells overexpressing ADH-A from *Rhodococcus ruber*, onto Supported Ionic Liquid Like Phases was developed. The efficiency of the corresponding biocatalyst can be finely tuned by considering different SILLPs loadings, pattern imidazolium substitutions and anion nature. The best results were obtained using a high loading resins based on hydrophilic cation and anion (methyl imidazole and chloride). The system is compatible with up to 30% v/v of DMSO allowing in this manner to increase the ketone concentration by using an organic cosolvent. Different aromatic and aliphatic ketones were efficiently reduced to the corresponding alcohols, the immobilised catalytic systems displaying good to very good conversions (60-89%) and excellent Prelog selectivities (99% ee). Finally, the excellent stability of the system was demonstrated when moving from batch to continuous flow conditions, obtaining high conversions in the bioreduction of acetophenone during a 120 h run with prolonged periods of storage. These result opens the application of supported ILs as non-conventional solid ionic solvents for immobilisation of redox biocatalytic systems.

Experimental section

General Information

Lyophilised cells of *E. coli* containing the expressed ADH was prepared as described in the literature.⁴³ All reagents were purchased from Sigma-Aldrich and used without further

purification. ¹H and ¹³C NMR experiments were carried out using a Bruker Avance III HD 400 MHz and Varian INOVA 500 MHz spectrometer. The chemical shifts are given in delta (δ) values (ppm). FTIR spectra were acquired with a MIRacle single-reflection ATR diamond/ZnSe accessory in a JASCO FT/IR-6200 instrument. Gas chromatography analyses were carried out in a GC VARIAN 3900 using a Sulpeco Beta Dex 120 column (30 m x 0.25 mm I.D. x 25 μm).

Synthesis and characterization of SILLPs.

The synthesis and characterization of SILLPs has been reported as previously described in the literature 12and 29

Immobilisation of ADH-A into SILLP.

Lyophilised cells of *E. coli* overexpressed ADH-A (100 mg) was suspended in 25 mL of Milli-Q H₂O, and the corresponding SILLP (1 g) was added. The suspension was shaken for 20 h at room temperature and 250 rpm to adsorb the enzyme. The supernatant was recovered, and the support was filtered and washed with Milli-Q H₂O (3 x 25 mL) to remove the non-adsorbed enzyme. The polymer was frozen at -15 °C and lyophilised.

Reduction of acetophenone (5a) in batch

The corresponding ADH-SILLP (50 mg) was suspended in 600 μL of Tris-HCl buffer (50 mM, pH 7.6), and then IPA (36 μL , 0.47 mmol, 0.68 M) and acetophenone (**5a**, 2.8 μL , 0.024 mmol, 40 mM) were added. The reaction mixture was shaken for 20 h at 200 rpm and 30 °C, and after this time, the reaction mixture was extracted with ethyl acetate (1 mL) and analysed by GC to calculate the yield of (*S*)-1-phenylethanol (**6a**). GC: SUPELCO-BDEX.meth Injector: 230 °C, Oven: 60 °C (0 min, step1), 60-130 °C (10 °C /min, step2), 130 °C (30 min, step3), Detector: 300 °C; (*R*)-1-phenylethanol (15.4 min) and (*S*)-1-phenylethanol (**6a**) (16.9 min)).⁴³

Reduction of acetophenone (5a) in DMSO (batch)

The ADH-SILLP-**2a**-Cl (50 mg) was suspended in 600 μL of a Tris-HCl buffer (50 mM, pH 7.6), DMSO (DMSO:buffer, 0-10% v/v), and then acetophenone (**5a**, 40-233 mM), and IPA (36 μL , 0.47 mmol, 0.68 M) were added. The reaction mixture was shaken for 20 h at 200 rpm and 30 °C, and after this time, the reaction mixture was extracted with ethyl acetate (1 mL) and analysed by GC to calculate the yield of (*S*)-1-phenylethanol (**6a**).

Reduction of ketones 5b-e in batch

The ADH-SILLP-**2a**-Cl (50 mg) was suspended in 600 μL of a Tris-HCl buffer (50 mM, pH 7.6), and then the corresponding ketone (**5b-e**, 0.024 mmol, 40 mM) and IPA (36 μL , 0.47 mmol, 0.68 M) were added. The reaction mixture was stirred at 200 r.p.m with orbital stirring at 30 °C. The reaction mixture was shaken for 20 h at 200 rpm and 30 °C, and after this time, the reaction mixture was extracted with ethyl acetate (1 mL) and analysed by GC to calculate the yield and enantiopurity of corresponding alcohol. 3'-Methoxyacetophenone (**5b**) (32.4 min) and (*S*)-1-(3-methoxyphenyl)ethan-1-ol (**6b**) (91.2 min). 4'-Bromoacetophenone (**5c**) (53.9 min) and (*S*)-1-(4-bromophenyl)ethan-1-ol (**6c**) (169.8 min). 2-Bromo-1-phenylethanol (**5d**) (8.4 min) and (*S*)-2-bromo-1-phenylethanol (**6d**) (52.5 min). Octan-2-one (**5e**) (3.2 min) and (*S*)-octan-2-ol (**6e**) (5.0 min).^{2,3}

Reduction of acetophenone (5a) in flow

Conditions I: A solution of acetophenone (**5a**, 60 μ L, 0.51 mmol, 40 mM), Tris-HCl buffer (12 mL, 50 mM, pH 7.6) and IPA (720 μ L, 9.45 mmol, 0.68 M) was pumped at 50 μ L/min through a fixed-bed reactor packed with 0.5 g of ADH-SILLP-**2a**-Cl at 40 $^{\circ}$ C.

Conditions II: A solution of acetophenone (**5a**, 64 μ L, 0.55 mmol, 40 mM), Tris-HCl buffer (12 mL, 50 mM, pH 7.6), IPA (720 μ L, 9.45 mmol, 0.68 M) and NADH (1 mL of a 10 mM solution of NADH in Tris-HCl buffer, 0.01 mmol, 0.73 mM) was pumped at 50 μ L/min through a fixed-bed reactor packed with 0.5 g of ADH-SILLP-**2a**-Cl at 40 $^{\circ}$ C.

Conditions III: A solution of acetophenone (**5a**, 512 μ L, 4.39 mmol, 40 mM), Tris-HCl buffer (96 mL, 50 mM, pH 7.6), IPA (5,76 mL, 75.33 mmol, 0.68 M) and NADH (8 mL of a 1 mM solution of NADH in Tris-HCl buffer, 0.008 mmol, 0.073 mM) was pumped at 50 μ L/min through a fixed-bed reactor packed with 0.5 g of ADH-SILLP-**2a**-Cl at 40 $^{\circ}$ C.

Aliquots were taken at different reaction times and extracted with ethyl acetate (1 mL). The samples were analysed by GC to calculate the yield of (S)-1-phenylethanol (**6a**).

Reduction of acetophenone (5a) in DMSO (flow)

A solution of acetophenone (**5a**, 793 μ L, 6.80 mmol, 71 mM) in Tris-HCl buffer (65 mL, 50 mM, pH 7.6), IPA (5.72 mL, 74.81 mmol, 0.77 M), DMSO (13 mL) and NADH (12.4 mL of a 10 mM solution of NADH in Tris-HCl buffer, 0.12 mmol, 1.28 mM) was pumped at 50 μ L/min through a fixed-bed reactor packed with 1 g of ADH-SILLP-**2a**-Cl at 40 $^{\circ}$ C. Aliquots were taken at different reaction times and extracted with ethyl acetate (1 mL). The samples were analysed by GC to calculate the yield of (S)-1-phenylethanol (**6a**).

Conflicts of interest

There are no conflicts to declare.

Acknowledgements

This work has been supported by RTI2018-098233-B-C22 and C21 and PID2019-109253RB-I00 (Spanish Ministry of Science and Innovation) 20790/PI/18 (Fundacion SENECA CARM) grants and UJI-B2019-40 (Pla de Promoció de la Investigació de la Universitat Jaume I). The authors are grateful to the SCIC of the Universitat Jaume I for technical support. The authors would like to thank Prof. Wolfgang Kroutil (University of Graz) for the generous gift of *E. coli* cells overexpressing ADH-A.

Notes and references

- 1 P.J. Dyson and P.G. Jessop, *Catal. Sci. Technol.* 2016, **6**, 3302.
- 2 a) F. van Rantwijk and R. A. Sheldon, *Chem. Rev.* 2007, **107**, 2757; b) P. Lozano, *Green Chem.* 2010, **12**, 555; c) M. K. Potdar, G. F. Kelso and L. Schwarz, C. Zhang, M. T. W. Hearn, *Molecules* 2015, **20**, 16788.
- 3 J.P. Hallett and T. Welton, *Chem. Rev.* 2011, **111**, 3508
- 4 T. Welton, *Biophys. Rev.* 2018, **10**, 691.
- 5 a) P. Lozano, T. De Diego, D. Carrie, M. Vaultier and J.L. Iborra, *Biotechnol. Lett.* 2001, **23**, 1529; b) P. Lozano, T. de Diego, J. P. Guegan, M. Vaultier and J. L. Iborra, *Biotechnol. Bioeng.* 2001, **75**, 563.
- 6 T. Itoh, *Chem. Rev.* 2017, **117**, 10567.
- 7 a) Sustainable Catalysis in Ionic Liquids, P. Lozano (Ed.). CRC. Press – Taylor & Francis, **2018**, Boca Ratón, b) P. Xu, S. Liang, M.-H. Zong, W.-Y. Lou, *Biotechn. Adv.*, 2021, 107702.
- 8 R *Supported ionic liquids: fundamentals and applications*, R. Fehrmann, A. Riisager and M. Haumann (Eds.), 1st edn., Wiley-VCH, Weinheim, **2014**.
- 9 C. Van Doorslaer, J. Wahlen, P. Mertens, K. Binnemans and D. De Vos, *Dalton Trans.* 2010, **39**, 8377.
- 10 E. García-Verdugo, B. Altava, M.I. Burguete, P. Lozano and S.V. Luis, *Green Chem.* 2015, **17**, 2693.
- 11 F. Giacalone, M. Gruttadauria, *ChemCatChem* 2016, **8**, 664.
- 12 V. Sans, N. Karbass, M.I. Burguete, V. Compañ, E. García-Verdugo, S.V. Luis and M. Pawlak, *Chem. Eur. J.* 2011, **17**, 1894.
- 13 A.Q. Pedro, J.A.P. Coutinho and M.G. Freire, *Immobilization of Ionic Liquids, Types of Materials, and Applications, Encyclopedia of Ionic Liquids*, 10.1007/978-981-10-6739-6_86-1, (1-12), **2019**.
- 14 S. Montolio, B. Altava, E. García-Verdugo and S. V. Luis, *Supported ILs and Materials Based on ILs for the Development of Green Synthetic Processes and Procedures*, in *Green Synthetic Processes and Procedures*, RSC Green Chemistry Series, ISBN: 978-1-78801-512-7, **2019**, p. 289.
- 15 a) J. Restrepo, P. Lozano, M.I. Burguete, E. García-Verdugo and S.V. Luis, *Catal. Today* 2015, **255**, 97; b) J. Restrepo, R. Porcar, P. Lozano, M.I. Burguete, E. García-Verdugo and S.V. Luis, *ACS Catal.* 2015, **5**, 4743

- 16 D. Valverde, R. Porcar, D. Izquierdo, M. I. Burguete, E. Garcia-Verdugo and S.V. Luis, *ChemSusChem* 2019, **12**, 3996
- 17 a) M.I. Burguete, E. García-Verdugo, I. Garcia-Villar, F. Gelat, P. Licence, S.V. Luis and V. Sans, *J. Catal.* 2010, **269**, 150; b) W. Gil, K. Boczon, A.M. Trzeciak, J. J. Ziótkowski, E. Garcia-Verdugo, S.V. Luis and V. Sans, *J. Mol. Cat. A: Chem.* 2009, **309**, 131.
- 18 a) P. Lozano, E. García-Verdugo, N. Karbass, K. Montague, T. De Diego, M.I. Burguete, and S.V. Luis, *Green Chem.* 2010, **12**, 1803; b) P. Lozano, E. García-Verdugo, J.M. Bernal, D.F. Izquierdo, M.I. Burguete, G. Sánchez-Gómez and S.V. Luis, *ChemSusChem* 2012, **5**, 790.
- 19 a) M.I. Burguete, H. Erythropel, E. Garcia-Verdugo, S.V. Luis and V. Sans, *Green Chem.* 2008, **10**, 401; b) S. Martín, R. Porcar, E. Peris, M.I. Burguete, E. García-Verdugo, S.V. Luis, *Green Chem.* 2014, **16**, 1639.
- 20 a) T. S. Moody, S. Mix, G. Brown and D. Beecher in *Science of Synthesis, Biocatalysis in Organic Synthesis*, Vol. 2, K. Faber, W.-D. Fessner, N. J. Turner (Eds.), Georg Thieme Verlag, Stuttgart, **2015**, p. 421; b) R. Zhang, Y. Xu and R. Xiao, *Biotechnol. Adv.*, 2015, **33**, 1671; c) F. Hollmann, D. J. Opperman and C. E. Paul, *Angew. Chem. Int. Ed.*, 2021, **60**, 5644
- 21 G. de Gonzalo, I. Lavandera, K. Durchschein, D. Wurm, K. Faber and W. Kroutil, *Tetrahedron Asymmetry*. 2007, **18**, 2541-2546. b) V. Gauchot, W. Kroutil and A. R. Schmitzer, *Chem. Eur. J.*, 2010, **16**, 6748; c) C. E. Paul, I. Lavandera, V. Gotor-Fernández and V. Gotor, *Top. Catal.*, 2014, **57**, 332.
- 22 a) M. Eckstein, M. Villela, A. Liese and U. Kragl, *Chem. Commun.* 2004, 1084-1085; b) S. Dreyer and U. Kragl, *Biotechnol. Bioeng.*, 2008, **99**, 1416-1424.
- 23 a) C. Kohlmann, S. Leuchs, L. Greiner, W. Leitner, *Green Chem.*, **2011**, **13**, 1430-1436; b) S. Leuchs, S. Na'amnieh, L. Greiner, *Green Chem.* **2013**, **15**, 167-176.
- 24 a) C. Shan, H. Yang, D. Han, Q. Zhang, A. Ivaska and L. Niu, *Biosensors and Bioelectronics*, 2010, **25**, 1504; b) A. Salimi, S. Lasghari and A. Noorbakhash, *Electroanalysis*, 2010, **22**, 1707; c) D. Zappi, S. Gabriele, L. Gontrani, D. Dini, C. Sadun, F. Marini and M. Letizia Antonelli, *Talanta*, 2019, **194**, 26.
- 25 W. Stampfer, B. Kosjek, C. Moitzi, W. Kroutil, K. Faber, *Angew. Chem. Int. Ed.* 2002, **41**, 1014; *Angew. Chem.* 2002, **114**, 1056.
- 26 a) K. Edegger, C. C. Gruber, T. M. Poessl, S. R. Wallner, I. Lavandera, K. Faber, F. Niehaus, J. Eck, R. Oehrlein, A. Hafner, and W. Kroutil, *Chem. Commun.* 2006, 2402; b) G. de Gonzalo, I. Lavandera, K. Faber, W. Kroutil, *Org. Lett.* 2007, **9**, 2163.
- 27 C. E. Paul, I. Lavandera, V. Gotor-Fernández, W. Kroutil and V. Gotor, *ChemCatChem*, 2013, **5**, 3875.
- 28 K. Goldberg, A. Krueger, T. Meinhardt, W. Kroutil, B. Mautner and A. Liese, *Tetrahedron: Asymmetry*, 2008, **19**, 1171.
- 29 M.I. Burguete, E. García-Verdugo, S.V. Luis and J.A. Restrepo, *Phys. Chem. Chem. Phys.* 2011, **13**, 14831.
- 30 The ADH/NADH redox system from *Rhodococcus ruber* was overexpressed in *Escherichia coli* strains. The cells of *E. coli* with the overexpressed ADH-A and cofactor were centrifuged and washed to yield a wet pellet, which was next resuspended in buffer and lyophilised to provide a solid powder. 4 mg/mL of this solid was suspended in buffer and offered to a gram of the corresponding SILLP. It should be noted that the soluble protein content obtained for the lyophilised cells of *E. coli* containing the expressed ADH was of 56 mg/100 mg of dry residue calculated after suspension of 40.9 mg of residue in 10 mL of Milli-Q H₂O at 200 rpm and 25 °C for 17 h. The soluble protein content was determined by Bradford test of supernatant obtained after centrifugation at 6 h and 1500 rpm.
- 31 This conversion is remarkable as, even using a molar excess of isopropanol 17 equiv regarding the ketone, the thermodynamic equilibrium is not completely shifted to the alcohol product.
- 32 E. S. Da Silva, V. Gómez-Vallejo, J. Llop and F. López-Gallego, *Catal. Sci. Technol.* 2015, **5**, 2705.
- 33 a) W. Stampfer, B. Kosjek, W. Kroutil and K. Faber, *Biotechnol. Bioeng.*, 2003, **81**, 865; b) M. Karabec, A. Lyskowski, K. C. Tauber, G. Steinkellner, W. Kroutil, G. Grogan and K. Gruber, *Chem. Commun.*, 2010, **46**, 6314
- 34 H. Gröger, W. Hummel, S. Buchholz, K. Drauz, T. Van Nguyen, C. Rollmann, H. Hüsken and K. Abokitse, *Org. Lett.* 2003, **5**, 173.

-
- 35 a) L. Olofsson, I.A. Nicholls and S. Wikman, *Org. Biomol. Chem.* 2005, **3**, 750; b) M. Wolberg, A. Ji, W. Hummel, M. Müller, *Synthesis* 2001, 937; c) I. Lavandera, A. Kern, M. Schaffenberger, J. Gross, A. Glieder, S. de Wildeman and W. Kroutil, *ChemSusChem* 2008, **1**, 431; d) G. Carrea and S. Riva, *Angew. Chem. Int. Ed.* 2000, **39**, 2226.
- 36 H. Hamada, T. Miura, H. Kumobayashi, T. Matsuda, T. Harada and K. Nakamura, *Biotechnol. Lett.* 2001, **23**, 1603.
- 37 N. Adebar and H. Gröger, *Bioengineering* **2019**, *6*, 99.
- 38 J. Döbber, M. Pohl, S. V. Ley and B. Musio, *React. Chem. Eng.*, 2018, **3**, 8.
- 39 F. Hildebrand and S. Lütz, *Tetrahedron: Asymmetry*, 2006, *17*, 3219.
- 40 a) P. Lozano, E. Garcia-Verdugo, S.V. Luis, M. Pucheault and M. Vaultier. *Curr. Org. Synth.* 2011, **13**, 4132; b) M. P. Thompson, I. Peñafiel, S. C. Cosgrove and N. J. Turner, *Org. Process. Res. Dev.* 2019, **23**, 9; c) A. I. Benítez-Mateos, M. L. Contente, D. R. Padrosa and F. Paradisi, *React. Chem. Eng.* 2021, **6**, 599; d) P. De Santis, L. E. Meyer, and S. Kara, *React. Chem. Eng.*, 2020, **5**, 2155.
- 41 B. Baumer, T. Classen, M. Pohl, J. Pietruszka, *Adv. Synth. Catal.* 2020, **362**, 2894.
- 42 J.M. Bolivar and F. López-Gallego, *Curr. Opin. Green Sustain. Chem.* 2020, **25**, 100349.
- 43 D. Méndez-Sánchez, J. Mangas-Sánchez, I. Lavandera, V. Gotor, and V. Gotor-Fernández, *ChemCatChem*, 2015, **7**, 4016.